Journal of Molecular Liquids 222 (2016) 963–971

Contents lists available at ScienceDirect

Journal of Molecular Liquids

journal homepage: www.elsevier.com/locate/molliq

Insights on self-aggregation phenomena of 1-indanone thiosemicarbazones and the formation of inclusion complexes with hydroxypropyl-β-cyclodextrin by Molecular Dynamics simulations

M. Florencia Martini [a,b,c], Romina J. Glisoni [b,c], Alejandro Sosnik [d], Albertina Moglioni [a,c], Mónica Pickholz [b,c,*]

[a] Universidad de Buenos Aires. CONICET. Instituto de Química y Metabolismo del Fármaco (IQUIMEFA). Buenos Aires, Argentina
[b] Universidad de Buenos Aires. CONICET. Instituto de Nanobiotecnología (NANOBIOTEC). Buenos Aires, Argentina
[c] National Science Research Council (CONICET), Argentina
[d] Laboratory of Pharmaceutical Nanomaterials Science, Department of Materials Science and Engineering, Technion-Israel Institute of Technology, Haifa, Israel

ARTICLE INFO

Article history:
Received 3 February 2016
Accepted 24 July 2016
Available online 27 July 2016

Keywords:
Molecular Dynamics
Cyclodextrins
Thiosemicarbazones of 1-indanone
Complex formation

ABSTRACT

1-Indanone thiosemicarbazones (TSCs) display a broad spectrum of pharmacological activities. However, their extremely poor solubility and self-aggregation tendency in water hurdles the reliable evaluation of the activity *in vitro*. To overcome these drawbacks, the formation of complexes with different natural and chemically modified cyclodextrins (CDs) has been investigated. Aiming to gain further insight into the molecular mechanisms involved in the interaction of these new chemical entities with CDs, this work investigated for the first time the interaction of two types of 1-indanone TSCs with hydroxyl-propyl-β-CD (HPβ-CD) by Molecular Dynamics (MD) simulations. Results were in good agreement with the experimental work and revealed the fundamental contribution of the substituents in the 1-indanone aromatic ring not only to the intrinsic aqueous solubility but also more importantly to the self-aggregation and the ability of the TSC to form stable complexes with the CD. In the particular case of the 5,6-dimethoxy-1-indanone derivative, the increase of the solubility in presence of HPβ-CD stems from a considerable decrease of the TSC-TSC intermolecular interactions and the formation of inclusion complexes that are stable for a short time. Then, the high self-aggregation tendency of this TSC destabilizes the complex and leads to the initial TSC insolubilization and subsequent precipitation.

1. Introduction

Since the potential therapeutic activity of thiosemicarbazones (TSCs) against *Mycobacterium tuberculosis* was described for the first time [1], many other pharmacological activities such as antibacterial [2], antiviral [3], antifungal [4], antiprotozoal [5] and antitumoral [6] have been reported. 1-Indanone TSC derivatives are effective against a broad spectrum of pathogens [7–10]. In particular, 5,6-dimethoxy-1-indanone TSC was more effective against the virus of the bovine viral diarrhoea (BVDV), the surrogate model of the hepatitis C virus (HCV) *in vitro*, than the first-line antiviral drug ribavirin [11,12]. However, these TSCs display extremely poor intrinsic aqueous solubility (1.5–13.0 μg/mL) [13]. In addition, 1-indanone TSCs combine a bulky hydrophobic aromatic ring and a highly hydrophilic thiosemicarbazone group (Fig. 1A). This peculiar structure confers the molecule amphiphilic character and it would account for the self-aggregation that leads to gradual nucleation, crystallization and precipitation in aqueous media [13]. This behaviour precluded the reproducible and reliable evaluation of the biological activity *in vitro* and gave place to inconsistent data of antiviral activity [13]. Moreover, it represents a hurdle toward the study of other antipathogenic properties. In this scenario, the investigation of new and complementary experimental and computational tools to elucidate drug self-aggregation and means to prevent and/or control it is called for.

Cyclodextrins (CDs) are macrocyclic oligosaccharides that consist of five or more α-D-glucopyranoside units tied with 1 → 4 glycosidic linkages. The shape of CDs resembles a truncated cone that combines a hydrophobic nano-sized cavity with a hydrophilic surface. The primary and secondary hydroxyl groups are located at the narrow and wide rim, respectively, of the CD ring (Fig. 1B). Since the cavity enables the partial or total incorporation of hydrophobic molecules that fit its size, CDs have found broad application in pharmaceutical research and development to increase the water solubility, physicochemical stability and bioavailability of lipophilic drugs through the formation of drug/CD inclusion complexes [14,15]. In addition, CDs have been more recently explored to increase the aqueous solubility of new chemical entities [16].

Following this concept, Glisoni et al. studied the solubilization and physical stabilization of 1-indanone TSCs in aqueous medium by

* Corresponding author at: NANOBIOTEC Universidad de Buenos Aires-Consejo Nacional de Investigaciones Científicas y Técnicas (UBA-CONICET), Buenos Aires, Argentina.
E-mail address: mpickholz@gmail.com (M. Pickholz).

http://dx.doi.org/10.1016/j.molliq.2016.07.109
0167-7322/

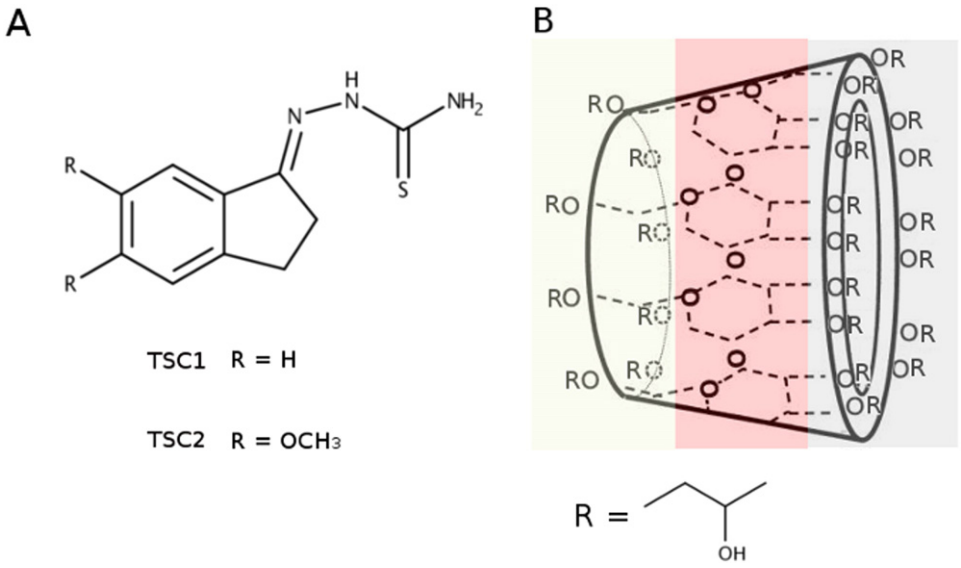

Fig. 1. Molecular structure of (A) 1-indanone-thiosemicarbazone (TSC1) and 5,6-dimethoxy-1-indanone-thiosemicarbazone (TSC2) and (B) 2-hydroxypropyl-β-cyclodextrin (HPβ-CD) included in the molecular dynamic (MD) simulations. The primary and secondary hydroxyl (—OH) groups and O atoms were colored in yellow and gray, respectively. The glycosidic oxygen bridges, which are directed toward the cavity inner space, were colored in light red. (For interpretation of the references to color in this figure legend, the reader is referred to the web version of this article.)

means of complexation with different natural and chemically modified CDs [17]. In this framework, with the water-soluble hydroxypropyl β-cyclodextrin (HPβ-CD), the solubility of 1-indanone TSC (TSC1, Fig. 1A) and 5,6-dimethoxy 1-indanone-TSC (TSC2, Fig. 1A) was increased up to 22 and 65 times, respectively. On the other hand, the TSC1/HPβ-CD complex was stable for at least one week, while the TSC2 counterpart underwent decomplexation after 24 h. The driving mechanism for the formation of a host-guest inclusion complex is the result of the interplay between energetic and entropic effects. Furthermore, from the experimental point of view, in many cases organic solvents are needed to promote their formation [18]. Then, the stabilization of such complexes depends on the establishment of Van der Waals and electrostatic interactions (especially the formation of H bonds). Expectedly, the extent of each contribution to the stabilization of the complex is associated with the chemical nature of the guest and the host molecules [19,20].

Molecular Dynamics (MD) simulation provides one of the most direct ways to theoretically investigate the molecular behaviour [21] of more complex systems (*e.g.*, guest-host interactions) that is not feasible by experimental approaches. In this framework, many research groups described MD simulations as a main tool for investigating CD inclusion complexes in aqueous medium to obtain a comprehensive model of complexation and molecular recognition phenomena [22–25].

Aiming to gain further insight into the molecular mechanisms involved in the interaction of 1-indanone TSCs with CDs, this work investigated for the first time the formation and stability of inclusion complexes of two potential anti-HCV agents, TSC1 and TSC2, with HPβ-CD by MD. In framework, two different approaches were employed. In the first one, 1:1 TSC:HPβ-CD complexes were pre-assembled at different relative orientations. In the second, cooperative effects were investigated. Overall results revealed the fundamental contribution of the substituents in the 1-indanone aromatic ring not only to the intrinsic aqueous solubility and self-aggregation behaviour but also, and more importantly, to the ability of the TSC to form stable complexes with the CD of choice.

1.1. Computational methods

To evaluate the guest-host interactions, two different types of systems were simulated: (i) 1:1 TSC:HPβ-CD (hydrated by 2060 water molecules) and (ii) 8:8 TSC:HPβ-CD (hydrated by 16,150 water molecules). In all the cases, the TSC concentration was 27 mM. Furthermore, the corresponding controls of the mentioned systems were studied to evaluate the behaviour of the TSC molecules in CD-free water.

All MD simulations were performed using the GROMACS 4.5 software package [26–28] and the GROMOS96 53a6 force field [29,30]. In this force field, the corresponding methylene and methyl groups were treated as a united atom type. The water molecule was modelled using the simple point charge (SPC) model [31]. Periodic boundary conditions in all directions were considered to minimize edge effects in a finite system. The electrostatic interactions were handled with the Smooth Particle Mesh Ewald (SPME) version of the Ewald sums [32,33]. The settings for the SPME method were a real space cut-off of 1.0 nm, a grid spacing of 0.12 nm and a cubic interpolation. In all the simulations, the Van der Waals interactions were cut off at 1.0 nm. The simulations were carried out in the NVT ensemble using the Berendsen thermostat [34]. The whole system was coupled to a temperature bath with a reference temperature of 300 K and a relaxation constant of 0.1 ps. No constraints were used for the bonds. The time step for the integration of the equation of motion was 1 fs. The non-bonded list was updated every 10 steps. To release steric clashes, 10^6 steepest descent cycles and 10^6 steps of conjugated gradient algorithm were carried out. Prior to the production run, a series of six equilibration steps of 1 ns each were performed upgrading the temperature progressively.

The ground-state geometry of TSC1 and TSC2 was optimized within the Density Functional Theory (DFT) using the B3LYP [35] functional and 6-31G* basis set. The partial atomic charges were obtained through a single point calculation employing the optimized geometries, at the Hartree-Fock level within the 6-31G* and the Merz-Singh-Kollman protocol [36]. All the quantum chemical calculations were carried out by means of the Gaussian package [37]. The force constants and intermolecular parameters were chosen in analogy to similar molecules already described by GROMOS. For 1:1 systems, TSC molecules were placed into the cavity of the HPβ-CD, either through the ring or through the nitrogenous tail, as explained below. Instead, the 8:8 simulated systems were built in a cubic box, using the Packmol package [38] sampling the TSC molecules in different and representative relative orientations. MD simulations were carried out up to 100 ns production run after the equilibration of the system. The images were obtained using Visual Molecular Dynamics [39] software (VMD from University of Illinois at Urbana-Champaign, IL, USA) and Grace [40] (xmgrace) software.

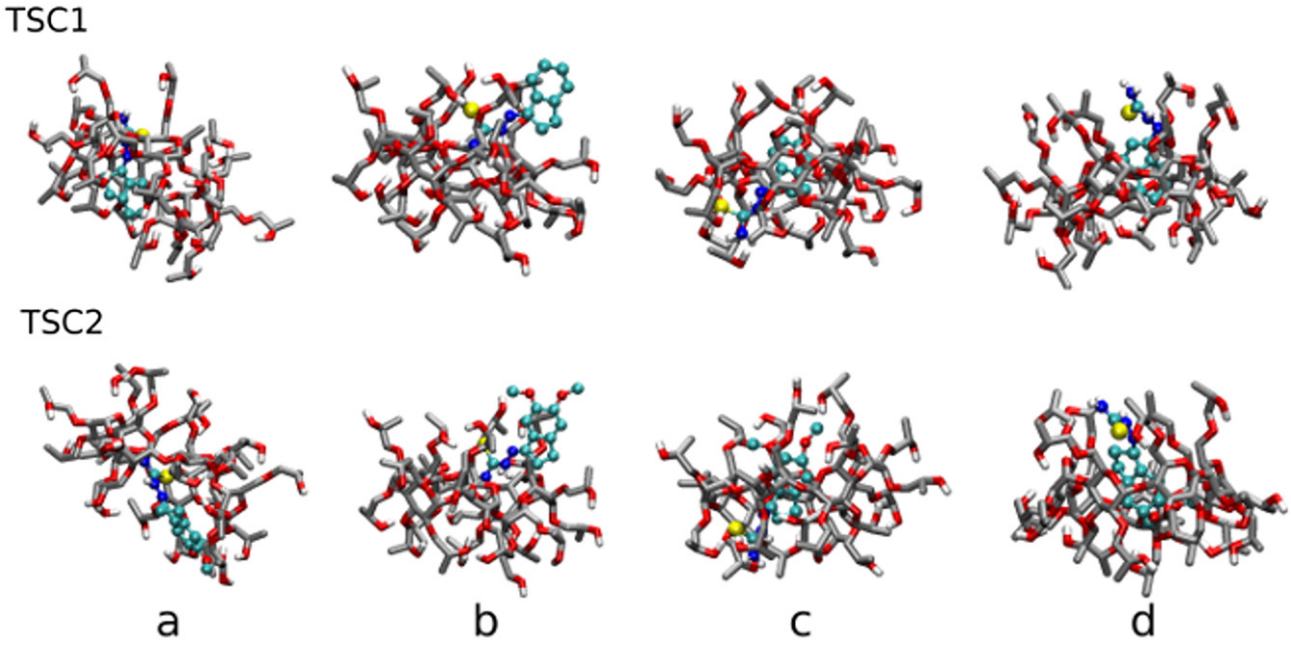

Fig. 2. Snapshots of the four initial positions of TSC1 and TSC2: (a) Nitrogenous tail inside the CD cavity and indanone group near the wider rim, (b) nitrogenous tail inside the CD cavity and indanone group near the narrower rim, (c) indanone group inside the CD cavity and nitrogenous tail near the wider rim, (d) indanone group inside the CD cavity and nitrogenous tail near the narrower rim of TSC1/HPβ-CD (upper panels) and TSC2/HPβ-CD (lower panels). Water molecules were not included here, for a better visualization.

2. Results and discussion

2.1. Inclusion complexes of TSC1 and TSC2 with HPβ-CD in water

Four different initial relative orientations for each TSC were studied and described: (a) the nitrogenous tail inside the CD cavity and the indanone group close to the wider rim, (b) the nitrogenous tail inside the CD cavity and the indanone group close to the narrower rim, (c) the indanone group inside the CD cavity and the nitrogenous tail close to the wider rim and (d) the indanone group inside the CD cavity and the nitrogenous tail near the narrower rim (Fig. 2).

The interaction energy, ΔE, between the host and the guest molecule could be an indication of the stability of the inclusion complexes. This parameter is typically defined as the sum of electrostatic (ΔE_{Coul}) and Van der Waals (ΔE_{LJ}) interaction energies [41,42] between guest and host molecules, according to Eq. (1).

$$\Delta E = \Delta E_{Coul} + \Delta E_{LJ} \tag{1}$$

Fig. 3 shows the interaction energy for the four 1:1 systems of TSC1 and TSC2 with HPβ-CD. Three types of stable complexes from the initial positions **a**, **b** and **c** (see above) were observed for both TSCs. For TSC1,

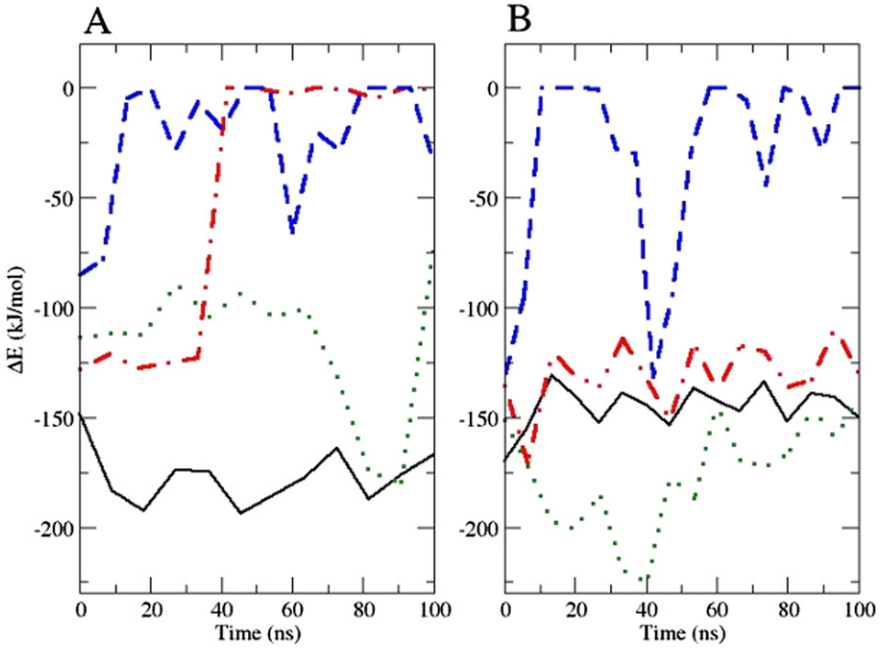

Fig. 3. Interaction energy between (A) TSC1 and (B) TSC2 with HPβ-CD in water *versus* simulation time of the four types of initial positions described in Fig. 2. Complex a (black), complex b (red), complex c (green) and complex d (blue). (For interpretation of the references to color in this figure legend, the reader is referred to the web version of this article.)

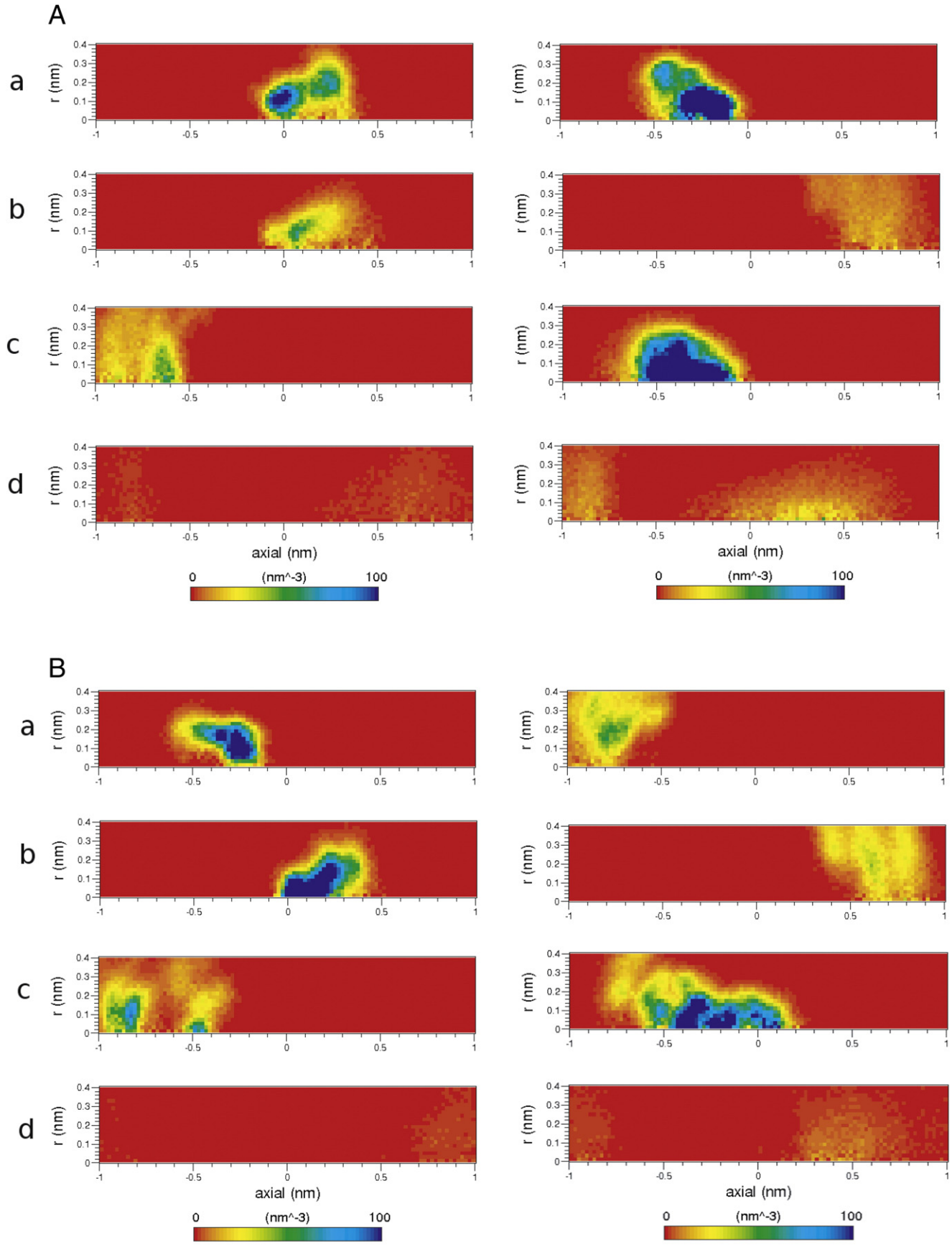

Fig. 4. Axial-radial number-density map of (A) TSC1 and (B) TSC2 indanone group (right panels) and nitrogenous tail (left panels) for the four different initial positions of 1:1 systems (a–d). Axial direction goes from the center of mass (CM) of the secondary hydroxyl groups to the CM of primary hydroxyl groups of the CD. Axial center is defined as the midpoint between the CMs of these two types of hydroxyl groups. (For interpretation of the references to color in this figure legend, the reader is referred to the web version of this article.)

the complex starting from position **a** was stable throughout the whole simulation time, while the complex **b** remained stable only for 30 ns and then the host molecule was released from the CD (Fig. 3A). In the case of TSC2, both inclusion complexes (**a** and **b**) turned out stable for the entire simulation time (Fig. 3B). In the case of complexes **c**, in both cases they showed a dual behaviour. TSC1 complex **c** remained stable during 60 ns, followed by a sharp peak of increase and decrease of ΔE. This observation would be related to the location of the indanone ring in a site of high steric hindrance (Fig. 3A). TSC2 also showed a different behaviour during the first 40 ns and the rest of the simulation time (Fig. 3B). Its analysis is detailed and discussed below.

In order to analyse the distribution of 1-indanone and TSC groups inside the HPβ-CD cavity, density maps of these residues were plotted considering cylindrical coordinates. The axial direction was defined by the vector going from the center of mass (CM) of the secondary –OH to the CM of the primary –OH of the HPβ-CD. The center (axial = 0) is defined as the geometrical midpoint between the CMs of these two types of –OH. These groups are separated ~0.5 nm from the CM, and the glycosidic oxygens are at ~0.4 nm of radial distribution (data not shown). Thereby, all the moieties observed between −0.5 nm and 0.5 nm of axial and 0 to 0.4 nm of radial distributions should be inside the CD cavity. The map of densities of each case is shown in Fig. 4, where the scale goes from red (absence) to blue (maximum average density) of the analysed group along the whole simulation time. As observed in Fig. 4A and in good agreement with the ΔE profile, the most stable complex was **a**. In this case, the whole molecule of TSC1 was found inside the CD cavity with its nitrogenous tail oriented to the primary –OH. For complex **b**, whose half-life time was shorter than that **a** and **c** (Fig. 3A), the nitrogenous tail was accommodated inside the CD cavity and close to the primary –OH. The complex **c** also showed good stability over most of the simulation time (Figs. 3A and 4A). In this case, the 1-indanone ring was placed in the widest portion of the cavity, and the nitrogenous tail outside the HPβ-CD. Otherwise, for complexes **a** and **b** of TSC2/HPβ-CD, the nitrogenous tail was placed within the CD cavity, either closer to the secondary or the primary –OH, respectively (Fig. 4B). It is important to mention that, for these two latter complexes, the indanone ring remains outside the HPβ-CD cavity (Fig. 4B). Conversely, in complex **c**, the 1-indanone system remained within the cavity, as observed for the TSC1/HPβ-CD complex (Fig. 4). During the first 40 ns, the TSC2 molecule was more deeply inserted into the CD cavity than the TSC1 counterpart, in a similar complex formation position (Fig. 4A). This phenomenon is essentially attributed to the H-bonds between the methoxy groups ($-OCH_3$) of TSC2 and the primary –OH of HPβ-CD and it is reflected in a higher value of $|\Delta E|$ than the complex **c** of TSC1. Finally, inclusion complex **d** showed no stability, regardless of the TSC (Fig. 4). Here, the steric hindrance precluded the incorporation of the 1-indanone residue into the narrower half of the HPβ-CD cavity. The primary and secondary rims of HPβ-CD present a difference in surface area of ~0.1 nm^2. Therefore, the penetration or stabilization of the guest molecule by the narrow rim of CD was constrained for both TSC derivatives (Table 1). In contrast, the 1-indanone residue was more easily hosted by the wider rim of HPβ-CD. At the same time, it is worth stressing that the molecular volume of both TSCs is smaller than that of the HPβ-CD cavity (Table 1). However, if the required surface area for access or permanence of a guest molecule inside the CD cavity is insufficient, the stabilization of any type of complex with the ring buried inside the narrowest portion of the CD cavity is not achieved.

Table 1
Sterical descriptors of the HPβ-CD cavity and TSC molecules.

Molecule	AWR (Å^2)	ANR (Å^2)	MPA (Å^2)	VC (Å^3)	vWV (Å^3)
HPβ-CD	44.2	33.18	–	304.5	–
TSC1	–	–	33.43	–	202.43
TSC2	–	–	43.91	–	254.59

Notes: AWR: Area of Wider Rim; ANR: Area of Narrower Rim; MPA: Minimal Projection Area; VC: Volume of cavity; vWV: van der Waals Volume.

Table 2
Mean number of H-bonds during inclusion complexes existence time, for each 1:1 system.

Guest-molecule	Initial Position	Interaction Range (ns)	Average H bond ± 0.1 (during interaction range)
TSC1	Complex-**a**	0–100	1.4
	Complex-**b**	0–38	1.4
	Complex-**c**	0–98	0.7
	Complex-**d**	0–10	0.5
TSC2	Complex-**a**	0–100	1.7
	Complex-**b**	0–100	1.5
	Complex-**c**	0–40/40–100	1.8/1.6
	Complex-**d**	30–50	0.8

2.2. Specific interactions

The stability of the inclusion complexes is given mainly by specific interactions between the guest and host molecule such as H-bonds. In this context, the average number of H-bonds during the lifetime of the different 1:1 inclusion complexes was measured (Table 2). As indicated, the strength of the H-bonds formed was slightly greater for TSC2/HPβ-CD than for TSC1/HPβ-CD complexes.

Taking into account the preliminary characterization of the inclusion complexes between TSCs and HPβ-CD molecules, but realizing that the differences found did not substantially justify their experimental singularities, we addressed the investigation of more complex systems consisting of eight molecules of TSC in water. These experiments assessed the collective properties of such molecules in the absence and presence of the respective eight molecules of HPβ-CDs. These experimental configurations are referred as 8:8 systems.

2.3. Collective properties of 8:8 TSC/HPβ-CD systems

In this part of the study, each pair was set up in one of the quadrants of the simulation box, having different (and representative) TSC:HPβ-CD relative orientations. These orientations were chosen to provide a robust sampling of the possible complexes under formation. To evaluate the behaviour of the TSC molecules in solution, we also simulated a system of eight TSC molecules in water (in the absence of HPβ-CD) and considered it as a control for comparative analyses. The systems were equilibrated in the same way described for 1:1 counterparts and the time simulation run was 100 ns that was long enough for the molecules to migrate and aggregate or disaggregate in solution. To study the self-aggregation behaviour of TSC molecules in the presence and absence of HPβ-CD, we estimated the average number of TSC neighbours (cut-off radius of 1 nm around each TSC molecule) that is a measure of the degree of molecular aggregation. In Fig. 5, we show the relative frequency of aggregation of TSC1 and TSC2, in absence and presence of HPβ-CD, respectively. In good correlation with the experimental findings, in the absence of HPβ-CD, the aggregation of TSC2 was substantially higher than TSC1 (Fig. 5A). In the presence of HPβ-CD, the number of TSC1 neighbours was not significantly modified with respect to the CD-free simulation (Fig. 5A). In contrast, TSC2 showed a striking decrease of the self-aggregation extent in the presence of HPβ-CD (Fig. 5B).

To study the dynamics of the self-aggregation process in the presence of the CD, we calculated the interaction energy between TSC molecules according to Eq. (1). As clearly observed in Fig. 6, the time evolution showed a gradual increase in the formation of TSC2 aggregates. This phenomenon was also appreciated experimentally [17], where TSC2 presented a faster and more substantial precipitation in water and consequently lower intrinsic solubility than TSC1 after complexation with HPβ-CD (Fig. 7) [17,43]. This latter effect could be attributed to the stronger tendency of TSC2 molecules to form π-π stacking interactions than TSC1, essentially driven by entropic effects. The different partial charge distribution in the

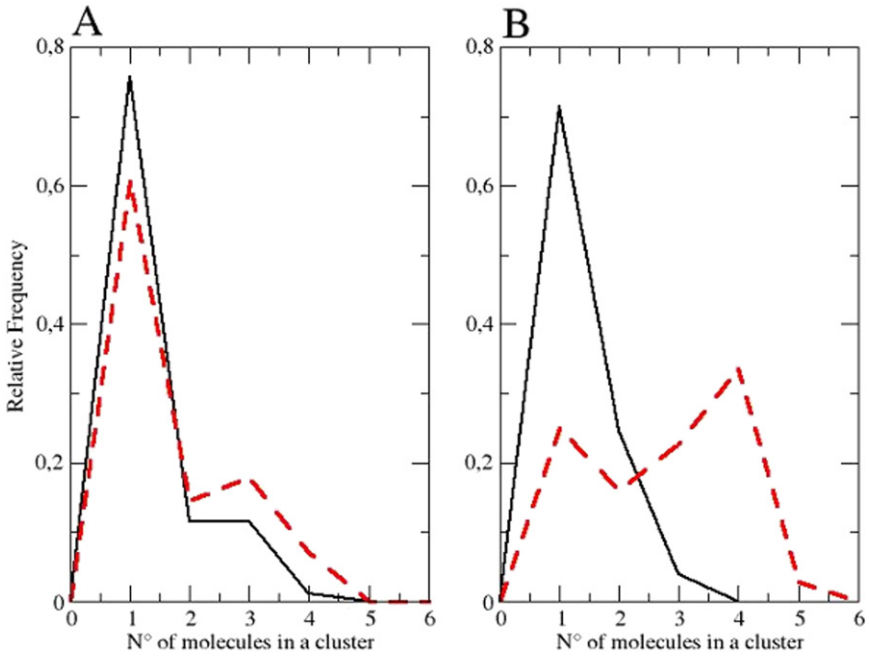

Fig. 5. Relative frequency of aggregation of (A) TSC1 and (B) TSC2, in the absence (red) and the presence (black) of HPβ-CD. (For interpretation of the references to color in this figure legend, the reader is referred to the web version of this article.)

aromatic carbons of the 1-indanone ring due to the presence of $-OCH_3$ substituents (data not shown) accounts for the differences between compounds. These electron-donating groups increase the ring electron density, favouring this type of interaction.

The high self-aggregation trend of TSC2 also disturbed the stabilization of the inclusion complex with the CD. Moreover, during the MD simulations and once the TSC2/HPβ-CD complex was formed, a negative cooperative effect over the complexation stabilization was evidenced. In this process, one TSC2 molecule belonging to an inclusion complex was released from the cavity of the HPβ-CD by a cooperative process mediated by many other free TSC2 molecules. This phenomenon finally led to TSC2-TSC2 interactions, as summarized in a selection of snapshots of Fig. 8. This evidence supported very well the experimental results reported elsewhere [13,17,43].

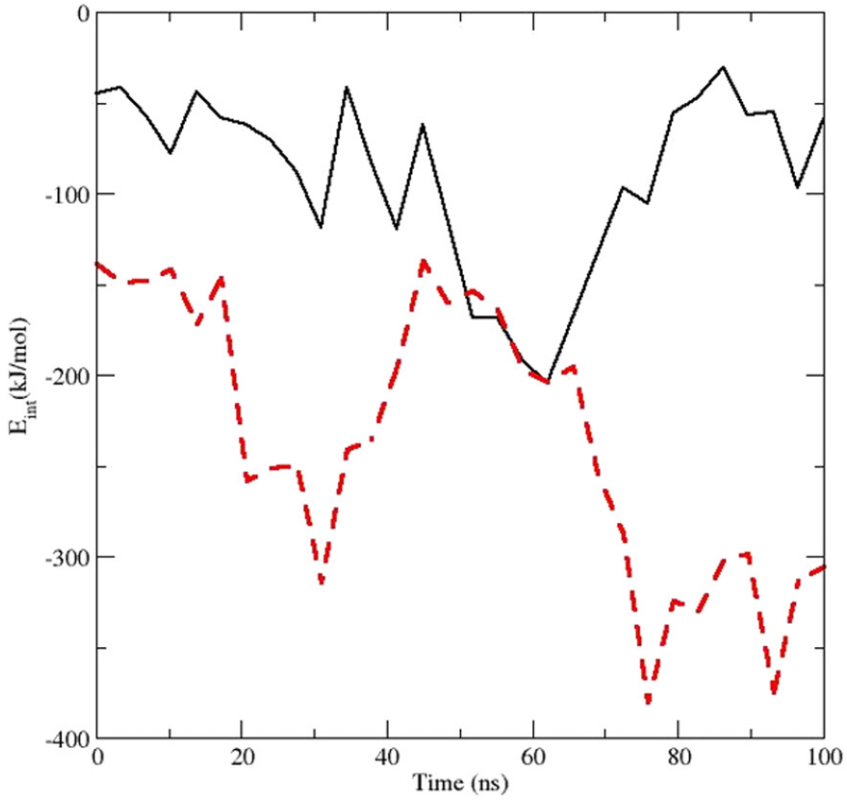

Fig. 6. Interaction energy between TSC molecules among themselves in systems where HPβ-CD molecules are present. TSC1 (black) and TSC2 (red). (For interpretation of the references to color in this figure legend, the reader is referred to the web version of this article.)

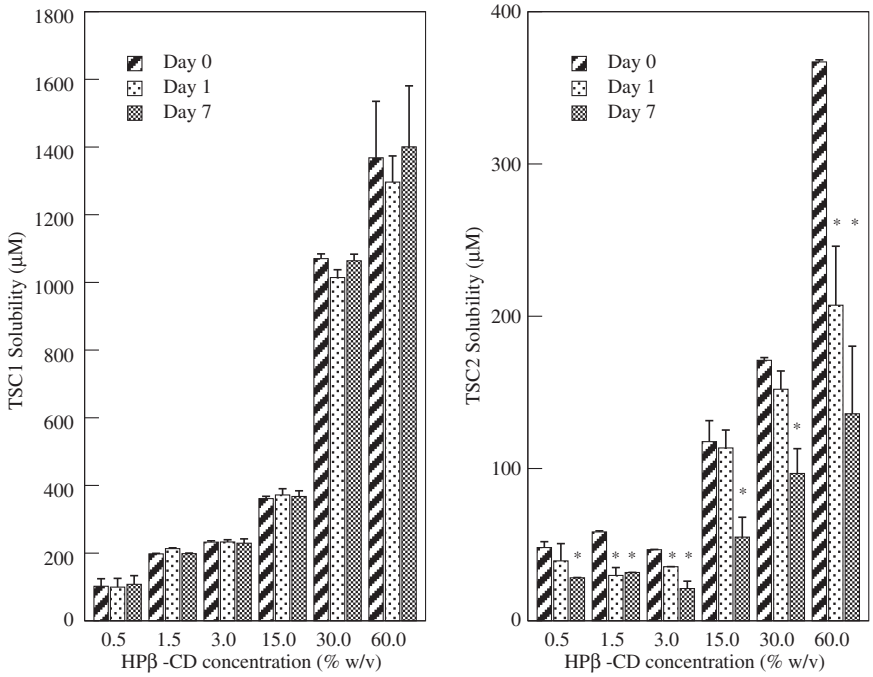

Fig. 7. Physical stability of (A) TSC1/HPβ-CD and (B) TSC2/HPβ-CD inclusion complexes in aqueous medium over 1 week, as estimated by TSC concentration at 25 °C. Results are expressed as mean value of three samples ± standard deviation (SD). *Statistically significant decrease of TSC concentration when compared to the TSC concentration in the inclusion complex at day 0 ($P < 0.05$). Note that the TSC1/HPβ-CD complex is stable in aqueous solution over time, as opposed to the TSC2/HPβ-CD counterpart. Figure 7B is reproduced from Reference [17] with permission of Springer.

2.4. Inclusion complexes formed in 8:8 systems

There was no *de novo* formation of inclusion complexes throughout the entire simulation, in any of the studied cases. In addition, it is worth pointing out that the experimental preparation of these complexes was conducted by the co-solvent method [17,18] to obtain a TSC/HPβ-CD white powder that was then resuspended in water to the desired CD concentration [17]. Moreover, results with dissolution or coprecipitation methods were not acceptable [43]. In this context, findings of the present work with both TSCs were in very good agreement with the experimental ones, where the molecules were incorporated into the CD cavity before they were exposed to the aqueous medium to prevent their early self-aggregation. This procedure ensured the formation of stable inclusion complexes and prevented early strong TSC-TSC interactions in water that result in the formation of pure TSC aggregates.

The stabilized inclusion complexes in the 8:8 systems were those in which the starting relative orientations were similar to those in the stable 1:1 complex. More specifically, the most stable structure of the complexes stabilized was similar to the one shown by complex **b** of 1:1 systems, for both types of TSCs (Fig. 9). TSC1 complexes were stable for 10 ns, while the TSC2 counterparts remained stable over ~70 ns. These differences were consistent with those found in complex **b** of the 1:1 systems. The shorter half-life of the TSC2 complex, in contrast with 1:1 system, could be explained by the effect of negative cooperativity of the complex stability, after it was formed (see above). As shown in Fig. 9, in both cases, the formation of inclusion complexes competed with that of non-inclusion ones. This means that TSC molecules are stabilized as non-aggregated entities outside the cavity through H-bond interactions with primary or secondary –OHs. The non-inclusion complex formation was more noticeable in the case of TSC1. This phenomenon could be related to the more significant increase of the intrinsic solubility in water and it would also explain why TSC1 water-solubilized in the presence of CDs was more stable over time than the TSC2 counterpart (Fig. 7) [17,43].

3. Conclusions

MD simulations were used to investigate the atomic-level phenomena and structural details of complexes that could be observed directly, stabilized between a chemically modified water-soluble β-CD (HPβ-CD) and two types of TSCs, 1-indanone and 5,6-dimethoxy-1-indanone TSC.

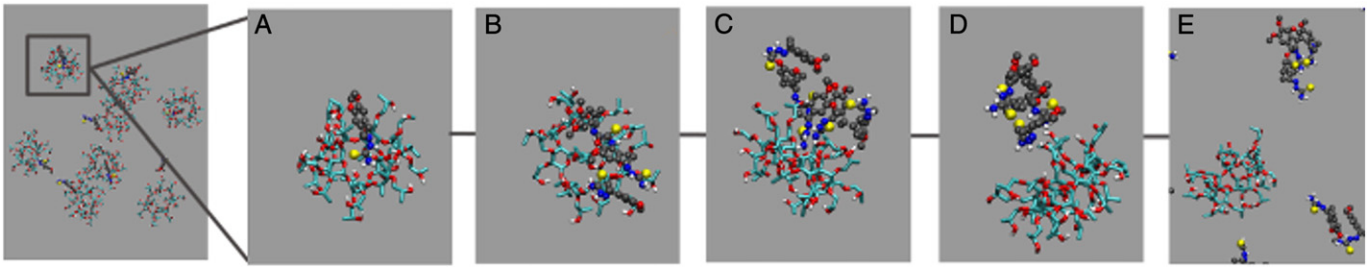

Fig. 8. Snapshots show the progress of the negative cooperativity of TSC2 on the aggregation process, at different simulation times. (A) $t = 0$ to 66 ns, (B) $t = 67$ ns, (C) $t = 72$ ns, (D) $t = 85$ ns and (E) $t = 88$ ns. The first snapshot shows the entire 8:8 system, the rest of them made zoom on the relevant part. Water molecules were not included here, for a better visualization.

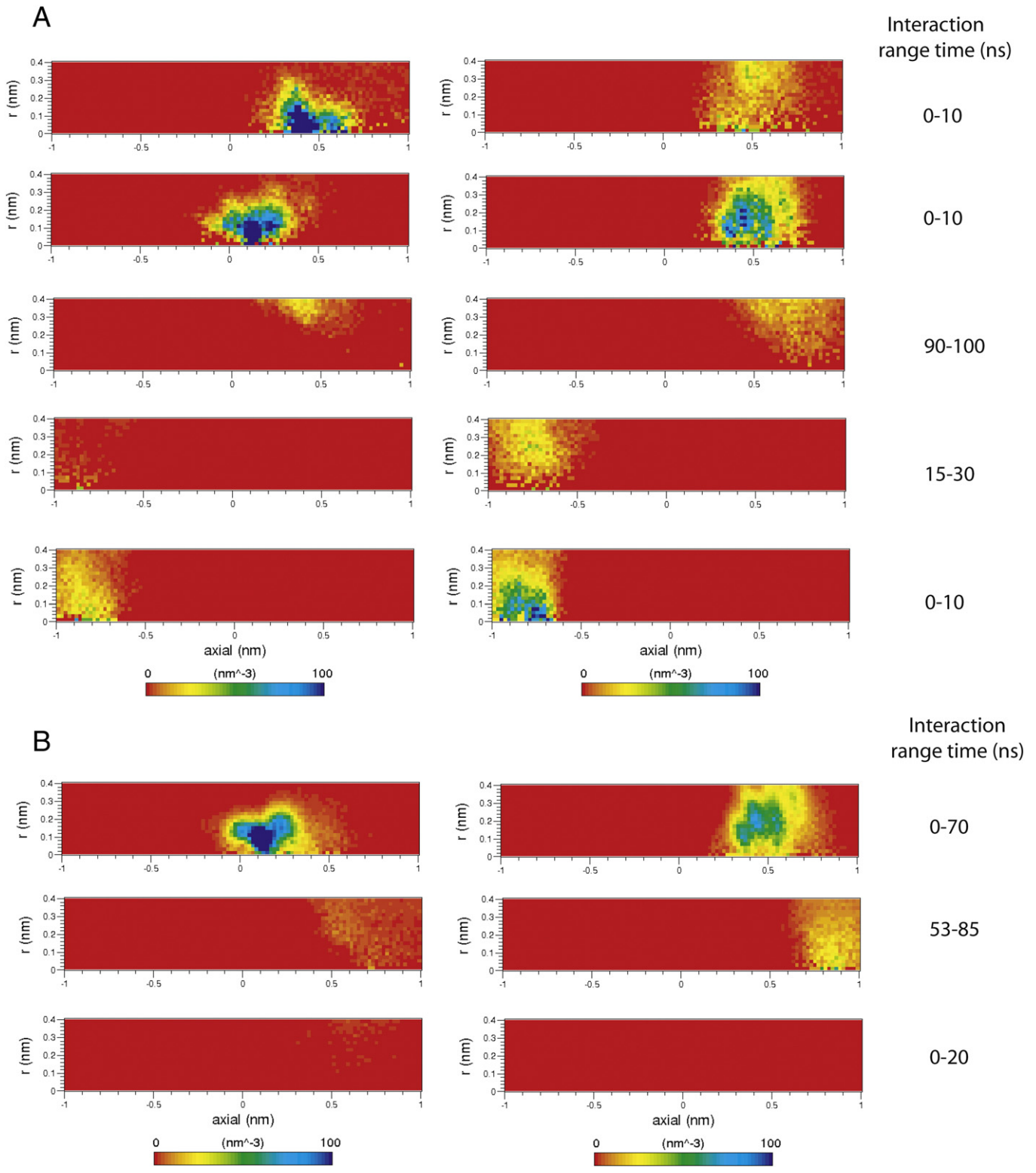

Fig. 9. Axial-radial number-density map of indanone group (right panels) and nitrogenous tail (left panels) for the inclusion and non-inclusion complexes formed during simulation time of 8:8 systems. (A) TSC1 and (B) TSC2. The axial direction goes from the center of mass (CM) of the secondary hydroxyl groups to the CM of primary hydroxyl groups of the CD. The axial center is defined as the midpoint between the CMs of these two types of hydroxyl groups.

Results were in good agreement with the experimental work and highlighted the strong impact that changes in the molecular structure of a drug (*e.g.*, incorporation of substituents to an aromatic heterocyclic ring) could have on the self-aggregation pattern and the formation of supramolecular assemblies with CDs. For instance, even though both TSC molecules showed higher aqueous solubility in the presence of HPβ-CD, the mechanism behind the solubilization is markedly different, as revealed from a molecular point of view. Furthermore, we found out that for both TSCs, only preformed inclusion complexes were stabilized. These findings support the production method used in previous experimental studies. Contrary to this, the formation of an inclusion complex between the CD and a hydrated TSC form could not be demonstrated.

Finally, the half-life of each complex was different. For TSC1, the increased solubility achieved in presence of HPβ-CD was by complex formation or disruption of TSC-TSC intermolecular interactions, and lasts over time due to the later formation of non- inclusion complexes. For TSC2, the increase in the solubility in presence of HPβ-CD was the result of a considerable decrease of the TSC2-TSC2 interactions, and the formation of inclusion complexes of TSC dehydrated molecules that were stable for a relatively short time, and followed by the reestablishment of TSC2-TSC2 interactions. This high self-aggregation tendency of TSC2 molecules destabilizes the complex and leads to initial TSC insolubilization and later precipitation, as observed experimentally.

Acknowledgments

This work was supported with funds from Agencia Nacional de Promoción Científica y Tecnológica (PICT 0706-2008, 310-2008), University of Buenos Aires (UBACYT 20020090200189, 20020100101063, B033,20020130200076BA) and CONICET (PIP0220, 11220100100401). MFM, RJG, AM and MP are members of the Research Career from Consejo Nacional de Investigaciones Científicas y Técnicas (CONICET, Argentina).

References

[1] G. Domagk, R. Behnisch, F. Mietzsch, H. Schimidt, On a new class of compounds effective in vitro against tubercle bacilli, Naturwissenschaften 33 (1946) 315–317.
[2] D. Sriram, P. Yogeeswari, P. Dhakla, P. Senthilkumar, D. Banerjee, N-Hydroxythiosemicarbazones: synthesis and in vitro antitubercular activity, Bioorg. Med. Chem. Lett 17 (2007) 1888–1891.
[3] G. Pelosi, F. Bisceglie, F. Bignami, P. Ronzi, P. Schiavone, M.C. Re, C. Casoli, E. Pilotti, Antiretroviral activity of thiosemicarbazone metal complexes, J. Med. Chem 53 (2010) 8765–8769.
[4] A.K. Halve, B. Bhashkar, V. Sharma, R. Bhadauria, A. Kankoriya, A. Soni, K. Tiwari, Synthesis and in vitro antimicrobial studies of some new 3-[phenyldiazenyl] benzaldehyde N-phenyl thiosemicarbazones, J. Enzyme Inhib. Med. Chem. 23 (2008) 77–81.
[5] X. Du, C. Guo, E. Hansell, P.S. Doyle, C.R. Caffrey, T.P. Holler, J.H. McKerrow, F.E. Cohen, Synthesis and structure–activity relationship study of potent trypanocidal thiosemicarbazone inhibitors of the trypanosomal cysteine protease cruzain, J. Med. Chem 45 (2002) 2695–2707.
[6] Z. Iakovidou, A. Papageorgiou, M.A. Demertzis, E. Mioglou, D. Mourelatos, A. Kotsis, Y.P. Nath, D. Kovala-Demertzi, Platinum(II) and palladium(II) complexes with 2-acetylpyridine thiosemicarbazone: cytogenetic and antineoplastic effects, Anti-Cancer Drugs 12 (2001) 65–70.
[7] C.C. García, B.N. Brousse, M.J. Carlucci, A.G. Moglioni, M. Martins Alho, G.Y. Moltrasio, N.B. D'Accorso, E.B. Damonte, Inhibitory effect of thiosemicarbazone derivatives on Junin virus replication in vitro, Antivir. Chem. Chemother. 14 (2003) 99–105.
[8] L.M. Finkielstein, E. Castro, L.E. Fabian, G.Y. Moltrasio, R.H. Campos, L.V. Cavallaro, A.G. Moglioni, New-1-indanone thiosemicarbazone derivatives active against BVDV, Eur. J. Med. Chem. 43 (2008) 1767–1773.
[9] E.F. Castro, L.E. Fabian, M.E. Caputto, D. Gagey, L.M. Finkielsztein, G.Y. Moltrasio, A.G. Moglioni, R.H. Campos, L.V. Cavallaro, Inhibition of bovine viral diarrhea virus RNA synthesis by thiosemicarbazone derived from 5,6-dimethoxy-1-indanone, J. Virol 85 (2011) 5436–5445.
[10] N. Gómez, D. Santos, R. Vázquez, L. Suescun, A. Mombrú, M. Vermeulen, L. Finkielsztein, C. Shayo, A. Moglioni, D. Gambino, C. Davio, Synthesis, structural characterization, and pro-apoptotic activity of 1-indanone thiosemicarbazone platinum(II) and palladium(II) complexes: potential as antileukemic agents, ChemMedChem 6 (2011) 1485–1494.
[11] R.J. Glisoni, E. Castro, L.V. Cavallaro, A. Moglioni, A. Sosnik, Complexation of a 1-indanone thiosemicarbazone with hydroxypropyl-ß-cyclodextrin enhances its activity against a hepatitis C virus surrogate model, J. Nanosci. Nanotechnol 15 (2015) 4224–4228.
[12] R.J. Glisoni, M.L. Cuestas, V. Mathet, J. Oubiña, A. Moglioni, A. Sosnik, Antiviral activity against the hepatitis C virus (HCV) of 1-indanone thiosemicarbazones and their inclusion complexes with hydroxypropyl-β-cyclodextrin, Eur. J. Pharm. Sci 47 (2012) 596–603.
[13] R. Glisoni, D.A. Chiappetta, L.M. Finkielstein, A.G. Moglioni, A. Sosnik, Self-aggregation behaviour of novel thiosemicarbazone drug candidates with potential antiviral activity, New J. Chem 34 (2010) 2047–2058.
[14] K.A. Connors, The stability of cyclodextrin complexes in solution, Chem. Rev. 97 (1997) 1325–1357.
[15] J. Szejtli, Introduction and general overview of cyclodextrin chemistry, Chem. Rev. 98 (1998) 1743–1754.
[16] H. Yang, M.A. Parniak, C.E. Isaacs, S.L. Hillier, L.C. Rohan, Characterization of cyclodextrin inclusion complexes of the anti-HIV non-nucleoside reverse transcriptase inhibitor UC781, AAPS J. 4 (2008) 606–613.
[17] R.J. Glisoni, D.A. Chiappetta, A.G. Moglioni, A. Sosnik, Novel 1-indanone thiosemicarbazone antiviral candidates: aqueous solubilization and physical stabilization by means of cyclodextrins, Pharm. Res 29 (2012) 739–755.
[18] E.M.M. del Valle, Cyclodextrins and their uses: a review, Process Biochem (39) (2004) 1033–1046.
[19] M.V. Rekharsky, Y. Inoue, Complexation thermodynamics of cyclodextrins, Chem. Rev. 98 (1998) 1875–1917.
[20] G. Raffaini, F. Ganazzoli, L. Malpezzi, C. Fuganti, G. Fronza, W. Panzeri, A. Mele, Validating a strategy for molecular dynamics simulations of cyclodextrin inclusion complexes through single-crystal X-ray and NMR experimental data: a case study, J. Phys. Chem. B 113 (2009) 9110–9122.
[21] V.P. Raut, M.A. Agashe, S.J. Stuart, R.A. Latour, Molecular dynamics simulations of peptide–surface interactions, Langmuir 21 (2005) 1629–1639.
[22] E. Cervelló, F. Mazzucchi, C. Jaime, Molecular mechanics and molecular dynamics calculations of the β-cyclodextrin inclusion complexes with m-, and p-nitrophenyl alkanoates, J. Mol. Struct. THEOCHEM 530 (2000) 155–163.
[23] K. Boonyarattanakalin, P. Wolschann, P. Toochinda, L. Lawtrakul, Molecular dynamics simulations of UC781-cyclodextrins inclusion complexes in aqueous solution, Eur. J. Pharm. Sci. 47 (2012) 752–758.
[24] H. Dodziuk, Cyclodextrins and Their Complexes: Chemistry, Analytical Methods, Applications, Wiley-VCH, Weinheim, 2006.
[25] B. Sellner, G. Zifferer, A. Kornherr, D. Krois, U.H. Brinker, Molecular dynamics simulations of β-cyclodextrin–aziadamantane complexes in water, J. Phys. Chem. B 112 (2008) 710–714.
[26] H.J.C. Berendsen, V. van der Spoel, R. van Drunen, GROMACS: a message-passing parallel molecular dynamics implementation, Comput. Phys. Commun 1-3 (1995) 43–56.
[27] D. Van Der Spoel, E. Lindahl, B. Hess, G. Groenhof, A.E. Mark, H.J.C. Berendsen, GROMACS: fast, flexible, and free, J. Comput. Chem 16 (2005) 1701–1718.
[28] B. Hess, C. Kutzner, D. van der Spoel, E. Lindhal, GROMACS 4: algorithms for highly efficient, load-balanced, and scalable molecular simulation, J. Chem. Theory Comput 3 (2008) 435–447.
[29] C. Oostenbrink, A. Villa, A.E. Mark, W.F. Van Gunsteren, A biomolecular force field based on the free enthalpy of hydration and solvation: the GROMOS force-field parameter sets 53A5 and 53A6, J. Comput. Chem 13 (2004) 1656–1676.
[30] I. Chandrasekhar, M. Kastenholz, R.D. Lins, C. Oostenbrink, L.D. Schuler, D.P. Tieleman, W.F. van Gunsteren, A consistent potential energy parameter set for lipids: dipalmitoylphosphatidylcholine as a benchmark of the GROMOS96 45A3 force field, Eur. Biophys. J 32 (2003) 67–77.
[31] J. Hermans, Interaction models for water in relation to protein hydration, in: H.J.C. Berendsen, J.P.M. Postma, W.F. van Gunsteren, Pullman (Eds.), Intermolecular Forces, Reidel, Dordrecht 1981, pp. 331–342.
[32] T. Darden, D. York, L. Pedersen, Particle mesh Ewald: an N·log(N) method for Ewald sums in large systems, J. Chem. Phys 12 (1993) 10089–10092.
[33] U. Essmann, L. Perera, M.L. Berkowitz, T. Darden, H. Lee, L.G. Pedersen, A smooth particle mesh Ewald method, J. Chem. Phys 19 (1995) 8577–8593.
[34] H.J.C. Berendsen, J.P.M. Postma, W.F. van Gunsteren, A. Dinola, J.R. Haak, Molecular dynamics with coupling to an external bath, J. Chem. Phys 8 (1984) 3684–3690.
[35] A.D. Becke, Density-functional thermochemistry. III. The role of exact exchange, J. Chem. Phys 98 (1993) 5648–5652.
[36] (a) U.C. Singh, P.A. Kollman, An approach to computing electrostatic charges for molecules, J. Comput. Chem 5 (1984) 129–145;
(b) P. Cieplak, P.A. Kollman, On the use of electrostatic potential derived charges in molecular mechanics force fields. The relative solvation free energy of cis- and trans-N-methyl-acetamide, J. Comput. Chem 12 (1991) 1232–1236.
[37] M.J. Frisch, G.W. Trucks, H.B. Schlegel, G.E. Scuseria, M.A. Robb, J.R. Cheeseman, V.G. Zakrzewski, J.J.A. Montgomery, R.E. Stratmann, J.C. Burant, S. Dapprich, J.M. Millam, A.D. Daniels, K.N. Kudin, M.C. Strain, O. Farkas, J. Tomasi, V. Barone, M. Cossi, R. Cammi, B. Mennucci, C. Pomelli, C. Adamo, S. Clifford, J. Ochterski, G.A. Petersson, P.Y. Ayala, Q. Cui, K. Morokuma, D.K. Malick, D. Rabuck, K. Raghavachari, J.B. Foresman, J. Cioslowski, J.V. Ortiz, B.B. Stefanov, G. Liu, A. Liashenko, P. Piskorz, I. Komaromi, R. Gomperts, R.L. Martin, D.J. Fox, T. Keith, M.A. Al-Laham, C.Y. Peng, A. Nanayakkara, C. Gonzalez, M. Challacombe, P.M.W. Gill, B. Johnson, W. Chen, M.W. Wong, J.L. Andres, C. Gonzalez, M. Head-Gordon, E.S. Replogle, J.A. Pople, GAUSSIAN98 (Revision A.7), Gaussian Inc., Pittsburgh, PA, 1998.
[38] J.M. Martínez, L. Martínez, Packing optimization for automated generation of complex system's initial configurations for molecular dynamics and docking, J. Comput. Chem 7 (2003) 819–825.
[39] W. Humphrey, A. Dalke, K. Schulten, VMD: visual molecular dynamics, J. Mol. Graph. 14 (1996) 33–38.
[40] Copyright (c) 1996–2008 Grace Development Team. Maintained by Evgeny Stambulchik.
[41] H. Zhang, W. Feng, C. Li, T. Tan, Investigation of the inclusions of puerarin and daidzin with β-cyclodextrin by molecular dynamics simulation, J. Phys. Chem. B 114 (2010) 4876–4883.
[42] M.A. Braga, M.F. Martini, M. Pickholz, F. Yokaichiya, M.K.D. Franco, L.F. Cabeça, V.A. Guilherme, C.M.G. Silva, C.E.G. Limia, E. de Paula, Clonidine complexation with hydroxypropyl-beta-cyclodextrin: from physico-chemical characterization to in vivo adjuvant effect in local anesthesia, J. Pharm. Biomed. Anal 119 (2016) 27–36.
[43] R.J. Glisoni, Aggregation and Complexation Studies of New Drugs Based on Thiosemicarbazones for the Evaluation of Their Biological ActivityPhD Thesis Faculty of Pharmacy and Biochemistry, University of Buenos Aires, 2012.